Open Access Full Text Article

ORIGINAL RESEARCH

The Anti-Breast Cancer Effect and Mechanism of Glimepiride-Metformin Adduct

Liangyuan Long[1–3]
Xiangnan Hu[1–3]
Xiaoli Li[1–3]
Duanfang Zhou[1–3]
Yun Shi [4]
Lingen Wang[5]
Hongfang Zeng[1–3]
Xiaoping Yu[1–3]
Weiying Zhou[1–3]

[1]College of Pharmacy, Chongqing Medical University, Chongqing 400016, People's Republic of China; [2]Chongqing Key Laboratory of Drug Metabolism, Chongqing 400016, People's Republic of China; [3]The Key Laboratory of Biochemistry and Molecular Pharmacology in Chongqing, Chongqing 400016, People's Republic of China; [4]West China Biopharm Research Institute, West China Hospital, Chengdu, Sichuan Province 610041, People's Republic of China; [5]Department of General Surgery, Leping People's Hospital, Leping, Jiangxi Province 333300, People's Republic of China

Correspondence: Weiying Zhou
College of Pharmacy, Chongqing Medical University, 1 Yixueyuan Road, Yuzhong District, Chongqing 400016, People's Republic of China
Tel/Fax +86 23 684 85161
Email wyzhou0118@163.com

Background: Compound adduct is a eutectic crystal formed by non-covalent bonds of two compounds or multiple compounds with water. Emerging evidence suggests that adduct could be different from the simple physical mixture of the individual compounds and has some new features. Recent studies reported that both glimepiride (Gli) and metformin (Met) may possess an anti-breast cancer effect besides anti-diabetic effect. In the current study, we synthesized glimepiride-metformin adduct (GMA) and examined its anti-breast cancer effect in vitro and in vivo to explore its potential in treatment of breast cancer in diabetic patients.

Methods: GMA was synthesized from Gli, Met and water at a molar molecular mass of 1:1:1 and identified by infrared spectroscopy. MTT assay, colony formation assay and wound healing assay were performed to examine the effects of GMA on cell viability and migration of human breast cancer cell lines CAL-148, MDA-MB-453, MDA-MB-231and MCF-7. The effect of GMA on cell cycle and apoptosis was examined by flow cytometry. The orthotopic implantation model was established to observe the inhibitory effect of GMA on tumor growth. The expression of Ki67 was detected by immunohistochemistry. RT-qPCR and Western blotting were performed to investigate mechanisms for the function of GMA.

Results: Both MTT and colony formation assays showed that GMA inhibited breast cancer cell viability, and the effect was greater than Gli alone, Met alone and the combination. In vivo study showed that GMA had an inhibitory effect on tumor growth of CAL-148 xenografts. Flow cytometry analysis indicated that GMA induced G1/S phase cell cycle arrest and apoptosis in breast cancer cells. RT-qPCR and Western blotting analyses showed that GMA activated AMPK, and up-regulated expression of p53 and p21, and down-regulated expression of cyclin D1 and CDK4.

Conclusion: GMA suppresses cell viability of breast cancer cells, and its effect is greater than Gli and Met alone or combination at the same concentration. GMA inhibits breast cancer cell growth in vivo. The antitumor effect of GMA may be related to the activation of AMPK resulting in up-regulation of p53 and p21 and down-regulation of cyclin D1 and CDK4.

Keywords: glimepiride, metformin, adduct, breast cancer, cell cycle, AMPK

Introduction

Breast cancer is the most common malignant tumor in women and the second leading cause of cancer death in female.[1] About 10–20% breast cancers are triple negative (ER-/PR-/HER-) and have no target therapy. Chemotherapy is one of the main methods for clinical treatment of triple negative breast cancer. However, the side effects and toxicity of chemotherapy drugs are big issues.[2] Therefore, finding alternative effective therapeutic drugs are of significance for triple negative breast cancer patients.[3]

3777

Metformin (Met) is a biguanide drug used to treat type 2 diabetes with poorly adjusted glycemic control after lifestyle adjustment.[4] In recent years, metformin has been reported to reduce the incidence of cancer and inhibit the growth of tumors including breast cancer, prostate cancer, ovarian cancer, liver cancer and so on.[5–8] Glimepiride (Gli) is a sulfonylurea drug used to treat type 2 diabetes.[9] It has been reported that glimepiride inhibits the proliferation of human breast cancer MCF-7 cells by down-regulating miRNA-34a expression,[10] indicating that glimepiride may have anti-breast cancer effect.

Compound adduct is a eutectic crystal formed by hydrogen bonds or non-covalent bonds of two compounds or multiple compounds. Emerging evidence suggests that adduct could be different from the simple physical mixture of the individual compounds,[11] and some adducts have a better antitumor effect than the simple physical mixture of the individual compounds. For example, rosiglitazone-metformin adduct has a better inhibitory effect on hepatocellular carcinoma than the physical mixture of rosiglitazone and metformin.[12] Glimepiride-metformin adduct (GMA) is a eutectic compound formed by non-covalent bonds in a molar molecular mass of 1:1:1 of glimepiride, metformin and water. Given that both Gli and Met had anti-breast cancer effect, we examined the effects of GMA on breast cancer and explored the potential in treatment of breast cancer, especially for diabetic breast cancer patients.

Materials and Methods
Reagents and Antibodies
Cell cycle and apoptosis analysis kit was purchased from Beytime Biotechnology (Shanghai, China). Glimepiride, metformin hydrochloride, paclitaxel and cisplatin were purchased from MedChemExpress (Monmouth Junction, NJ, USA). Rabbit antibodies to β-actin, phospho-AMPKα, AMPKα, phospho-p53, p53, p21, phospho-cyclin D1, cyclin D1, CDK4 were purchased from Cell Signaling Technology (Beverly, MA, USA).

Synthesis and Infrared Spectrum Detection of GMA
Gli (4 mmol) and Met free base (4 mmol) were collected in a round bottom flask, adding 70 mL absolute ethanol. Then, the mixture was heated at 70~80°C for 15 min under the condition of continuously whisking. After filtration, the liquid was distilled for removal of ethanol with a rotating evaporator and cooled down. At last, GMA

was obtained after recrystallized from absolute ethanol (2.00 g, yield 83%, melting point: 122–125°C).[13] For infrared spectrum detection of GMA, each compound (1 mg) was ground into powder with dried KBr (50 mg) in a mortar. The mixture was pressed into a piece of slice and tested in an infrared spectrometer (Nicolet, USA).

Cell Culture
The human triple negative breast cancer cell lines CAL-148, MDA-MB-453 and MDA-MB-231 and ER+ breast cancer cell line MCF-7 were purchased from American Type Culture Collection (ATCC). MCF-7 cells and MDA-MB-231 cells were cultured in DMEM (HyClone Corp., Logan, UT, USA) supplemented with 10% FBS (HyClone Corp., Logan, UT, USA) and antibiotics (100 U/mL penicillin and 0.1 mg/mL streptomycin) under 37°C and 5% CO_2 humidified condition. CAL-148 and MDA-MB-453 cells were cultured in RPMI 1640 medium (HyClone Corp., Logan, UT, USA) supplemented with 10% FBS and 1% penicillin/streptomycin (Beytime Biotechnology, Shanghai, China) under 37°C and 5% CO_2 humidified condition.

MTT Assay
MTT [3-(4,5-dimethylthiazol-2-yl)-2,5-diphenyl-2Htetrazoliumbromide] assay was used to measure cell viability. Cells were seeded at 1×10^4 cells/well in 96-well plates and treated with Gli, Met, or GMA at different concentrations (0.025, 0.05, 0.1, 0.2, 0.4 mM) for 48 h. Then, the medium was removed from cells and replaced with the 5 mg/mL MTT solution. After incubation for 4 h, MTT solution was discarded and 150 μL dimethyl sulfoxide (DMSO) was added to dissolve the formazan dye trapped in the living cells. The optical density (OD) values were detected at 570 nm with a microplate reader (Thermo Fisher Scientific, Waltham, MA, USA), and the inhibition rate was calculated.

Colony Formation Assay
Cells were seeded at 200 cells/well into 96-well cell culture plates with 3 replicates per group. After the cells were adherent, they were treated with the drugs, and the culture was terminated after 10 days of drug treatment. The medium was aspirated, and the cells were washed twice with PBS, fixed with 4% paraformaldehyde for 10 minutes, and stained with crystal violet (Beytime Biotechnology, Shanghai, China). The colonies containing 50 cells or

more were counted under a microscope (Nikon, Japan), and the colony formation rate was calculated.

Wound Healing Assay

CAL-148 cells were seeded in a 6-well plate at a density of 5.0×10^5/well. When the cell density was above 95%, the tip uniformly scratched along the bottom with a 200 μL pipette tip, and washed twice with PBS. The negative control group was added with a medium containing no serum and antibiotics, and the drug-administrated group was added with the same medium and treated with drugs. After incubation at 37°C, 5% CO_2 incubator for 0 h, 24 h, 48 h, and 72 h, the cells were observed under a microscope (Nikon, Japan) and images were captured. The experiment was performed in triplicate. The migration distance of the cells was analyzed using ImageJ 1.8 software, and the cell migration rate was calculated.

Cell Cycle and Apoptosis Detection

CAL-148 cells and MDA-MB-453 cells were treated with GMA at different concentrations (0.1, 0.2, 0.4 mM) for 48 h. For cell cycle analysis, the cells were collected, fixed, and incubated with propidium iodide (PI) staining solution in the dark for 30 min. Cell cycle distribution was analyzed by flow cytometry (Beckman Coulter, USA) from Academy of Life Sciences (Chongqing Medical University, China). For cell apoptosis analysis, the cells were harvested and washed twice with cold PBS. The cells were resuspended in Annexin V binding buffer, and then stained with Annexin V-FITC solution and propidium iodide (PI) solution for 15 min in the dark. The stained cells were analyzed by flow cytometry.

Orthotopic Implantation Model Analysis

Four-week-old female BALB/c-nude mice were purchased from Laboratory Animal Services Center of Chongqing Medical University. Mice were maintained under specific pathogen-free (SPF) conditions. Experiments were performed in accordance with national guidelines for animal care and use, and approved by the Animal Care and Use Committee of Chongqing Medical University. An orthotopic implantation model was established in nude mice at the fourth breast mammary fat pad with CAL-148 cells (2.5×10^6 cells/50μL). When tumors had grown to approximately 100 mm³, sixteen mice bearing the xenograft were randomly divided into four groups (4 mice/group): the control group (15 mg/kg carboxymethyl cellulose, oral gavage), metformin group (200 mg/kg, oral gavage), low

dose GMA group (200 mg/kg, oral gavage) and high dose GMA group (400 mg/kg, oral gavage). Mice were gavaged with drugs every day, and tumor size and mice weight were measured every 4 days after treatment. Tumor volume (V) was calculated using the following formula: $V (mm^3) = 0.5 \times (length \times width^2)$. Mice were sacrificed after treatment for 3 weeks, and tumor tissues were harvested.

Immunohistochemistry (IHC)

Tumor sections were dewaxed, soaked in ethanol, and then blocked with 3% H_2O_2. A specific immunoreactivity was blocked with diluted normal rabbit serum at room temperature. Sections were then incubated overnight at 4°C with specific primary antibody diluted in blocking buffer. After being washed with PBS, sections were further incubated with biotinylated secondary antibody (diluted 1:50), stained with a freshly prepared diaminobenzidine solution, and then counterstained with Mayer's hematoxylin.

Reverse Transcription and Quantitative Real-Time PCR (RT-qPCR)

Total RNA was extracted from tumor tissues using Trizol reagent (Life Technologies Corporation, USA). RNA reverse transcription was processed following the manufacturer's instructions by using a Reverse Transcription Kit (Takara, Japan). Then, qPCR was performed using TB Green Fast qPCR Mix Kit (Takara, Japan). The primer sequences were as follows: p53:forward 5′-GCTGGCATTTGCACCTACCT -3′ and reverse 5′-ACTACCAACCCACCGACCAA-3′; p21: forward 5′-TACCTCAG GCAGCTCAAGCA-3′ and reverse 5′-GACTCCACCCGATGACAGTT-3′; β-actin: forward 5′-GGACTTCGAGCAAGAGATGG-3′ and reverse 5′-CGATTTGAGG GGCCAGTGTC-3′. β-actin was used as an internal control. All primers were synthesized by Sangon Biotechnology. The relative mRNA levels were determined using the $2^{-\Delta\Delta CT}$ method.

Western Blotting

The total proteins were extracted with RIPA lysis buffer and protein concentrations were measured with a BCA protein-assay kit (Beytime Biotechnology, Shanghai, China). Subsequently, proteins were separated by SDS-PAGE and transferred to nitrocellulose (NC) membranes (Millipore, Billerica, MA, USA). After blocking with 5% non-fat milk for 2 h at room temperature, the membrane was incubated with the primary antibody overnight at 4°C, and then

incubating with the secondary antibody for 2 h at room temperature. The bands were visualized by chemiluminescence reagents (GE Healthcare life science, USA), and imaged using a ChemiDoc XRS (Bio-Rad, Hercules, CA, USA).

Statistical Analysis

Experiments were performed in triplicate unless indicated, and all the results are presented as means ± SD. Data were analyzed by Student's *t*-test or ANOVA, and $p < 0.05$ was considered statistically significant.

Results

IR Spectrum Analysis of Glimepiride-Metformin Adduct

The structure of Gli, Met, the mixture of Gli and Met, and GMA were examined by IR spectrum analysis, and the characteristic absorption peaks are shown in Table 1. Gli

Table 1 Infrared Spectrum Analyses for Gli, Met, the Mixture of Gli and Met, and GMA

Chemical Bonds and Functional Groups	Absorption Peaks (cm^{-1})
Glimepiride	
N–H bond in sulfonyl and carbonyl	3369
–NH bond in carbonyl and aromatic rings	3288
–NH bond in carbonyl	3136
C=O bonds in sulfonyl and lactam	1708, 1673
Metformin Hydrochloride	
NH$_2$ vibration	3166
N–H vibration	3371
C=NH vibration	1626
N–H bending vibration	1584, 1567
Symmetrical bending vibration	1448, 1418
Dimethyl asymmetric vibration	1475
The Mixture of Glimepiride and Metformin Hydrochloride	
N–H vibration	3371
N–H bond in sulfonyl and carbonyl	3369
–NH bond in carbonyl and aromatic rings	3290
–NH bond in carbonyl	3155
C=O bonds in sulfonyl and lactam	1707, 1673
C=NH vibration	1626
NH$_2$ vibration	3155
Glimepiride-Metformin Adduct	
N–H vibration	3381
C=O bonds in sulfonyl and lactam	1704, 1665

possessed N–H bond in sulfonyl and carbonyl, -NH bond in carbonyl and aromatic rings, -NH bond in carbonyl, C=O bonds in sulfonyl and lactam (absorption peaks at 3369, 3288, 3136, 1708, 1673 cm^{-1}) (Figure 1A). Met possessed NH$_2$ vibration, N–H vibration, C=NH vibration, N–H bending vibration, Symmetrical bending vibration, Dimethyl asymmetric vibration (absorption peaks at 3166, 3371, 1626, 1584, 1567, 1448, 1418, 1475 cm^{-1}) (Figure 1B). IR spectrum of the Gli and Met mixture showed that absorption peaks of Gli and Met in the mixture did not move and no new characteristic peaks were generated, indicating that the physical mixture of Gli and Met is a simple addition or overlap of Gli with Met, with no chemical bond formation (Figure 1C). In contrast, the IR spectrum of GMA indicated that C=O vibrations of sulfonyl and lactam of Gli moved toward low-frequency vibration in GMA and generated sharp peaks at 1704, 1665 cm^{-1}, and NH vibration of Met moved toward high-frequency vibration in GMA and generated sharp peaks at 3381 cm^{-1} (Figure 1D). These data confirmed that GMA is a novel adduct consisting of Gli and Met, instead of a simple physical mixture of Gli and Met.

Effects of GMA on Cell Viability and Colony Formation of Breast Cancer Cells

Given that both Gli and Met alone have anti-breast cancer effect, we first tested whether GMA has anti-breast cancer effect. MTT assay showed that GMA dose-dependently inhibited the proliferation of ER+ positive breast cancer cell line MCF-7, and triple negative breast cancer cell lines MDA-MB-231, CAL-148 and MDA-MB-453 (Figure 2A–D). In CAL-148 and MDA-MB-453 cells, 0.4 mM GMA could achieve over 50% inhibition on cell viability (Figure 2C and D). We then compared the effect between GMA and Gli, Met or their combination. As shown in Figure 2E and F, the inhibitory effect of GMA was greater than that of Met and Gli alone or the combination at the same concentration.

Colony formation assay also showed that GMA significantly inhibited colony formation of MDA-MB-453 and CAL-148 cells, and the inhibitory effect of GMA was greater than that of Met alone or Met combined with Gli at the same concentration (Figure 3A–C).

We then tested the effect of the combination of GMA and chemotherapy drugs paclitaxel or cisplatin on viability of breast cancer cells. Combination of 0.2 mM GMA with paclitaxel or cisplatin did not have
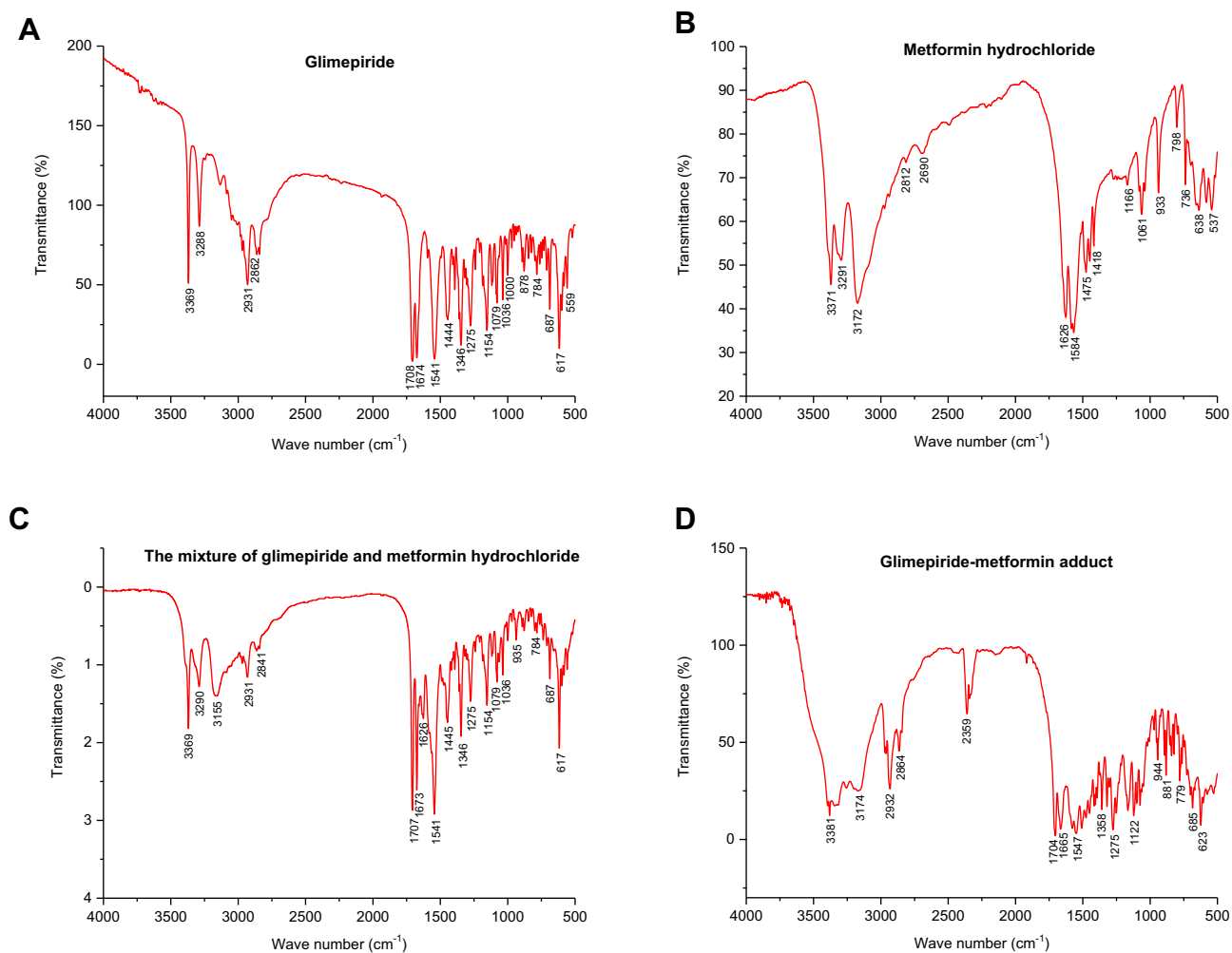
Figure 1 The infrared spectroscopy analysis results of Gli, Met, the mixture of Gli and Met, and GMA. (**A**) Gli. (**B**) Met. (**C**) The mixture of Gli and Met. (**D**) GMA.

a synergistic effect but had greater inhibitory effect on viability of CAL-148 and MDA-MB-453 cells than the chemotherapy agents alone, or GMA alone (Figure 4A–D), suggesting that GMA can enhance paclitaxel or cisplatin effects on breast cancer.

Effect of GMA on Migration of Breast Cancer Cells

We then tested whether GMA had an effect on migration of breast cancer cells. Wound healing assay was performed after CAL-148 cells were treated with Met alone or combination with Gli, or GMA. The results showed that GMA significantly restrained the migration of CAL-148 cells compared with Met alone and Met combined with Gli (Figure 5A and B), suggesting that GMA can inhibit migration of breast cancer cells.

GMA Induces G1/S Phase Cell Cycle Arrest

Given that GMA inhibits cell viability of breast cancer cells, we performed flow cytometry to examine the effects of GMA on cell cycle and apoptosis in MDA-MB-453 and CAL-148 cells. To this end, MDA-MB-453 and CAL-148 cells were treated with different concentrations (0.1, 0.2, 0.4 mM) of GMA for 48 hours. As shown in Figure 6A–C, GMA dose-dependently increased G0/G1 phase and reduced S phase in both CAL-148 and MDA-MB-453 cells, suggesting that GMA induces G1/S phase cell cycle arrest. As contrast, only 0.4 mM GMA significantly induced apoptosis compared to the control ($p < 0.05$), and the increased apoptosis rates were only about 5% in MDA-MB-453 cells and about 3% in CAL-148 cells (Figure 7A–D), respectively, suggesting that the effect of GMA on
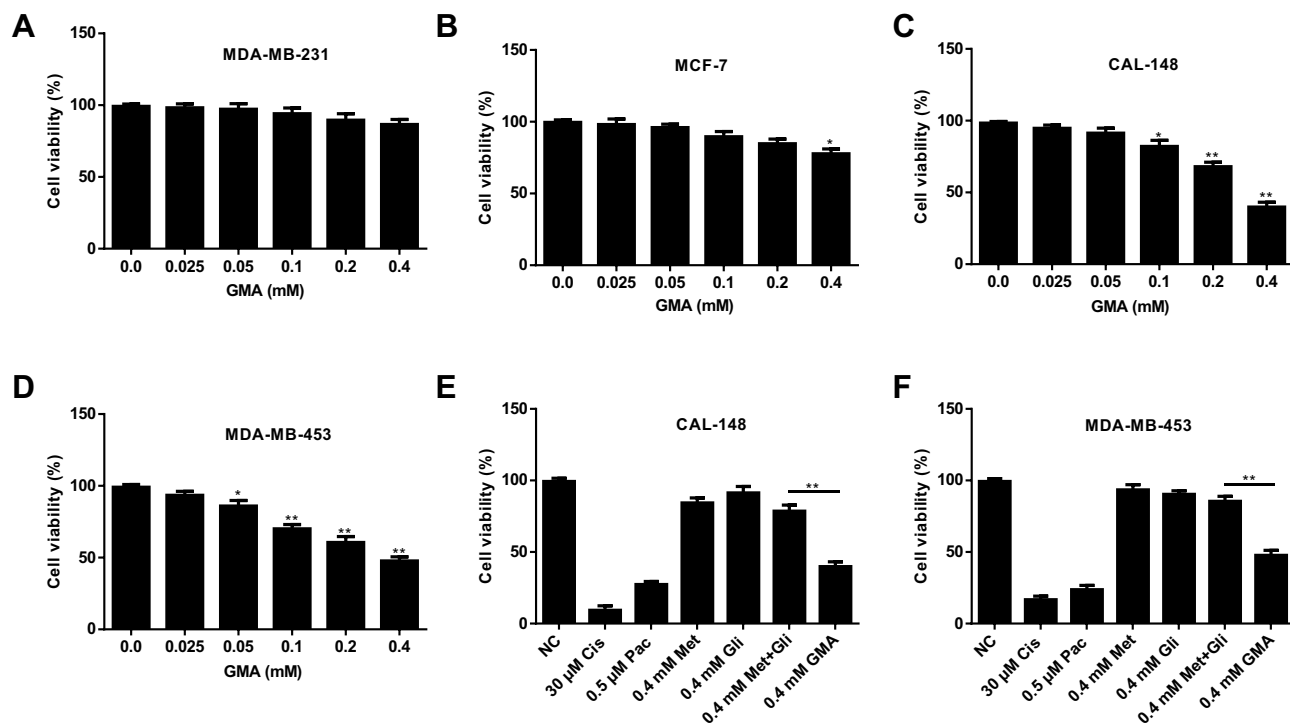
Figure 2 Effect of GMA on cell viability of breast cancer cells. (**A–D**) MDA-MB-231, MCF-7, CAL-148 and MDA-MB-453 cells were treated with different concentrations of GMA as indicated for 48 h. Cell viability was detected by MTT assay and inhibition rate was calculated. *$p < 0.05$ and **$p < 0.01$ versus the control group. N=3. (**E, F**) CAL-148 and MDA-MB-453 cells were treated with 30 μM Cisplatin (Cis), 0.5 μM Paclitaxel (Pac), 0.4 mM Met, 0.4 mM Gli, the mixture of 0.4 mM Gli and 0.4 mM Met, and 0.4 mM GMA for 48 h. Cell viability was measured by MTT assay and inhibition rate was calculated. Chemotherapy drugs Cis and Pac serve as the positive control. **$p < 0.01$. N=3.
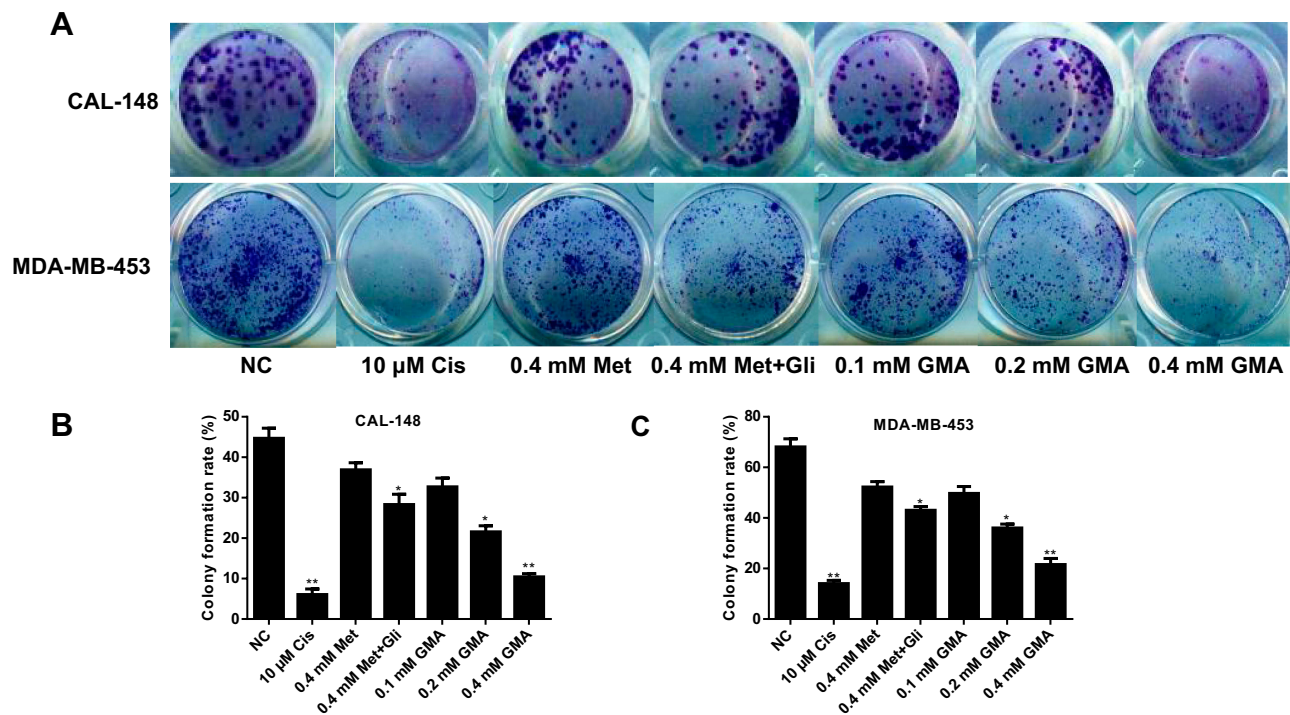
Figure 3 Effect of GMA on colony formation of breast cancer cells. (**A**) CAL-148 cells and MDA-MB-453 cells were treated with 10 μM cisplatin, 0.4 mM Met, 0.4 mM Met plus 0.4 mM Gli, or increasing concentrations of GMA as indicated, respectively. Cells were fixed and stained with crystal violet. (**B, C**) Quantitative results of colony formation assays by CAL-148 cells (**B**) and MDA-MB-453 cells (**C**) were displayed. *$p < 0.05$ and **$p < 0.01$ versus the control group. N=3.
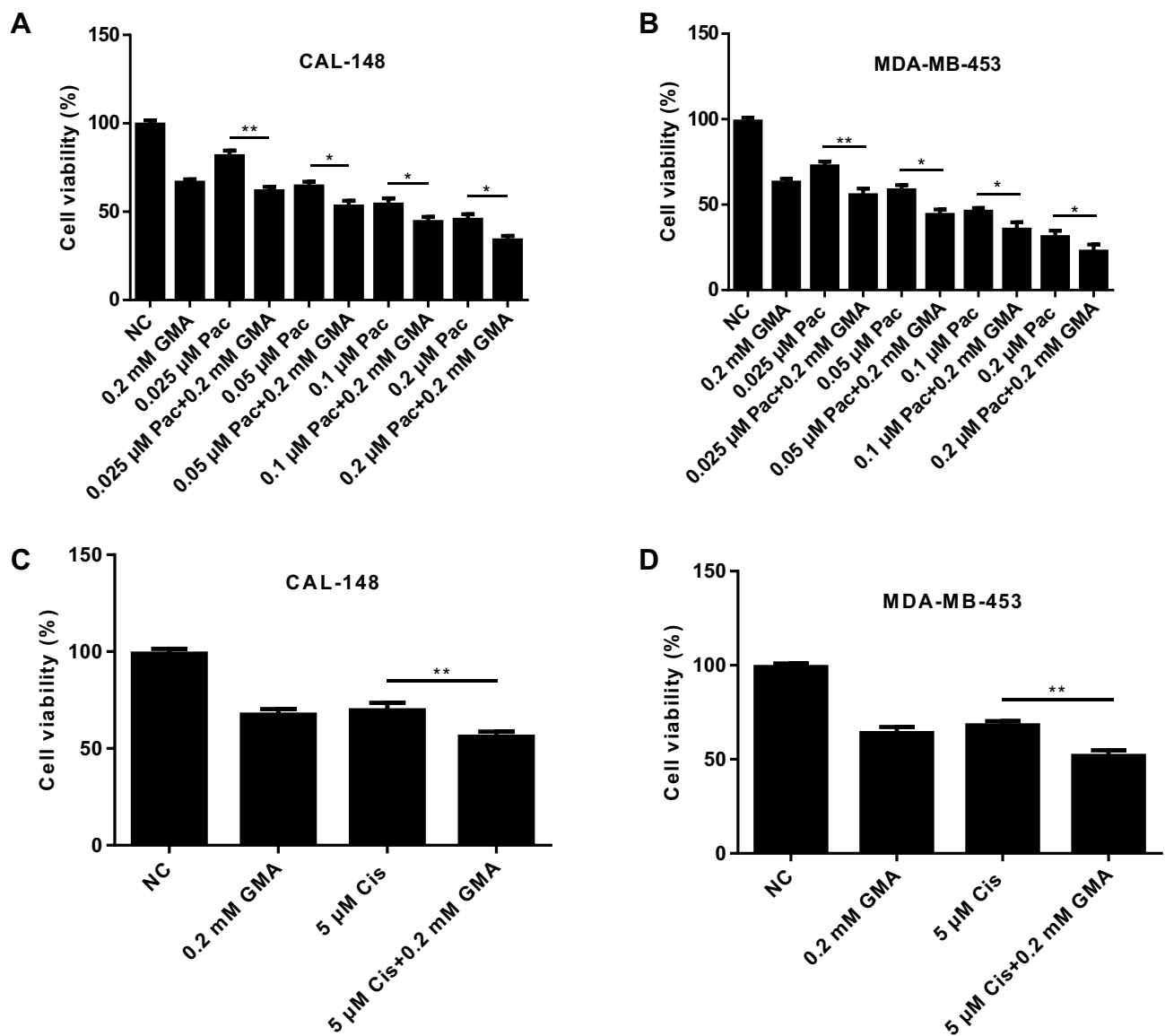
Figure 4 GMA enhances antitumor effect of chemotherapy drugs in breast cancer cells. (**A, B**) CAL-148 and MDA-MB-453 cells were treated with different concentrations of Paclitaxel alone or plus 0.2 mM GMA for 48 h. Cell viability was measured by MTT assay and inhibition rate was calculated. *$p < 0.05$ and **$p < 0.01$. (**C, D**) CAL-148 and MDA-MB-453 cells were treated with 5 μM cisplatin alone or plus 0.2 mM GMA for 48 h. Cell viability was measured by MTT assay and inhibition rate was calculated. **$p < 0.01$. N=3.

apoptosis of MDA-MB-453 and CAL-148 cells was moderate. Together, the data suggest that GMA inhibits breast cancer cell viability mainly through induction of G1/S phase cell cycle arrest.

GMA Suppresses Tumor Growth in vivo

Next, we investigated whether GMA inhibits breast cancer tumor growth in vivo. To this end, CAL-148 cells were injected into female nude mice. After breast cancer xenografts were developed, the nude mice bearing CAL-148 xenografts were randomly divided into four groups and daily administrated with carboxymethyl cellulose (the

control group), metformin (200 mg/kg), low dose GMA (200 mg/kg) and high dose GMA (400 mg/kg) by oral gavage. After 3 weeks, nude mice were sacrificed and the tumors in each group were harvested for examination. We found that high dose GMA group had significantly smaller tumor volume and lower tumor weight compared with the control group, while the low dose GMA group also reduced the tumor volume and weight compared with control group but it did not reach statistically significant (Figure 8A–C). To evaluate the safety, the body weight of mice was measured. No significant reduction in body weight was found in high dose GMA group and low
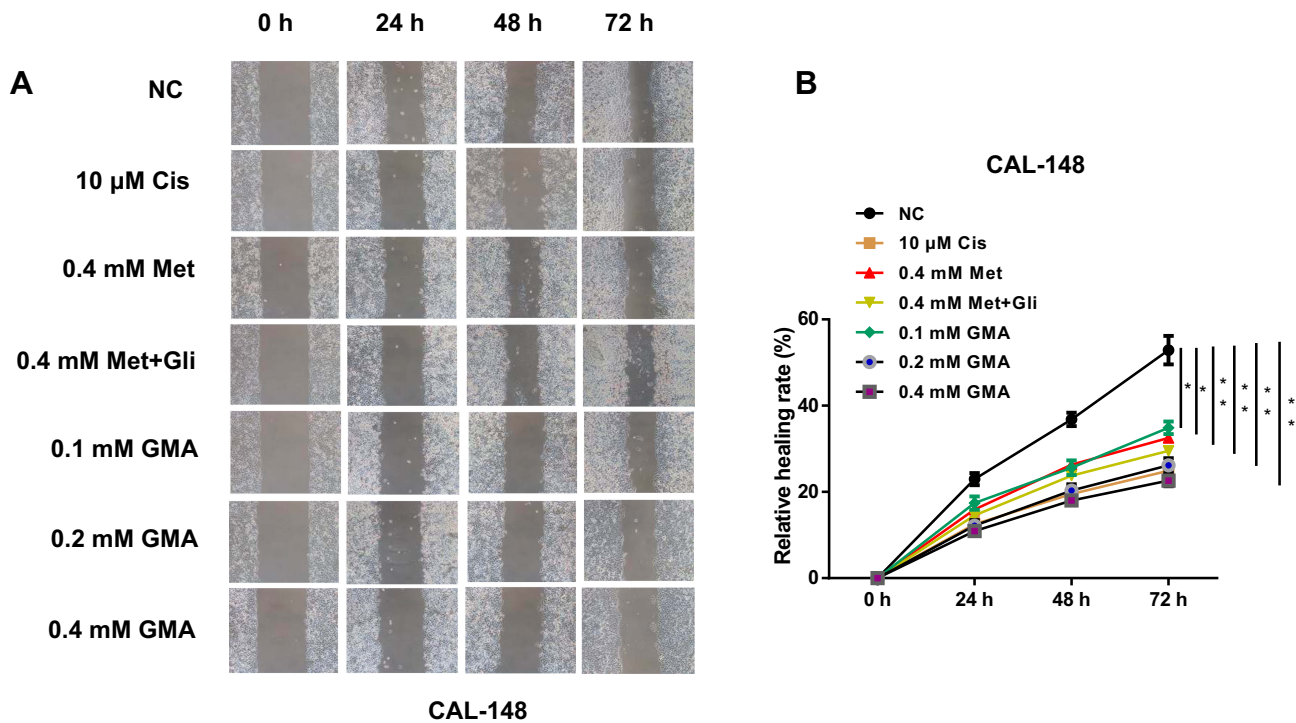
Figure 5 Effect of GMA on cell migration of breast cancer. (**A**) Nearly confluent CAL-148 cells were uniformly scratched by pipette tip and then treated with 10 μM cisplatin, 0.4 mM Met, 0.4 mM Met plus 0.4 mM Gli, or increasing concentrations of GMA as indicated. The effect of GMA on the migratory ability of CAL-148 cells was detected by wound healing assays. (**B**) Quantification of wound healing by CAL-148 was displayed. *$p < 0.05$ and **$p < 0.01$ versus the control group. N=3.
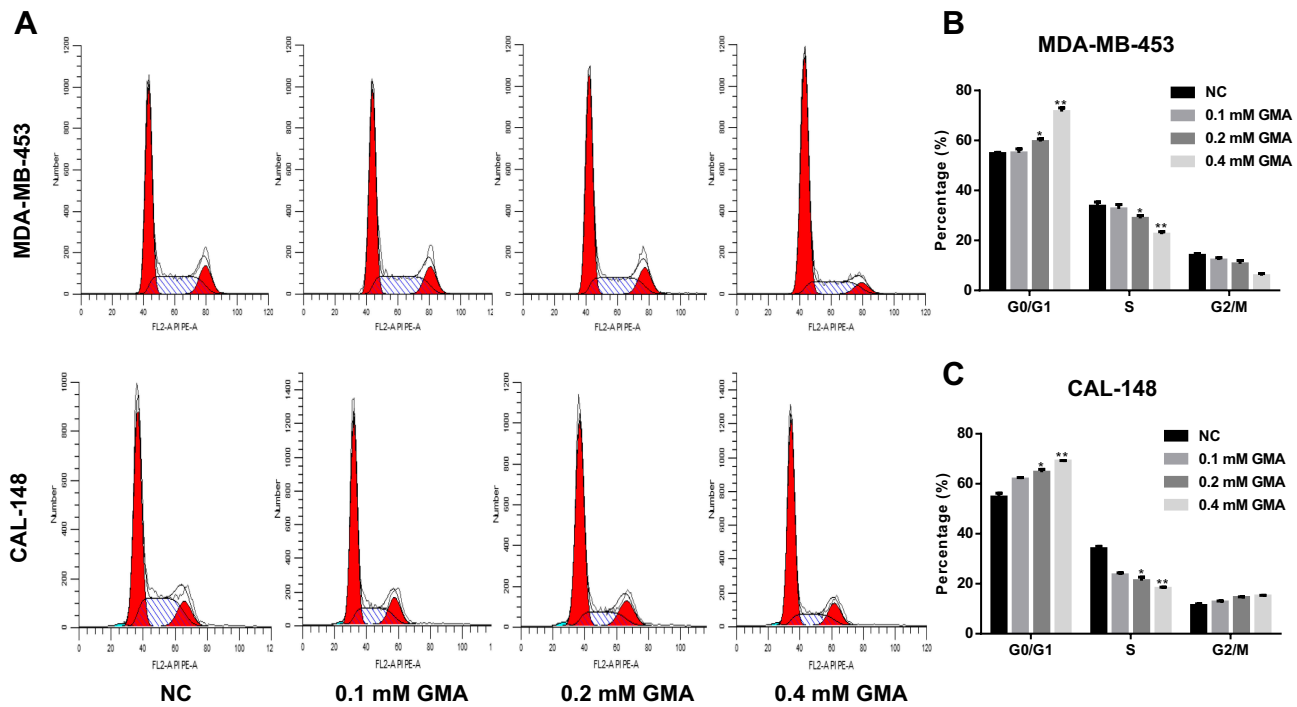

Figure 6 Effect of GMA on cell cycle of CAL-148 and MDA-MB-453 cells. (**A**) MDA-MB-453 and CAL-148 cells were treated with different concentrations of GMA, respectively. After 48 hours of treatment, cells were harvested for flow cytometric analysis to detect cell cycle. (**B**) Quantitative cell cycle analysis results of MDA-MB-453 cells. (**C**) Quantitative cell cycle analysis results of CAL-148 cells. *$p < 0.05$ and **$p < 0.01$ versus the control group. N=3.
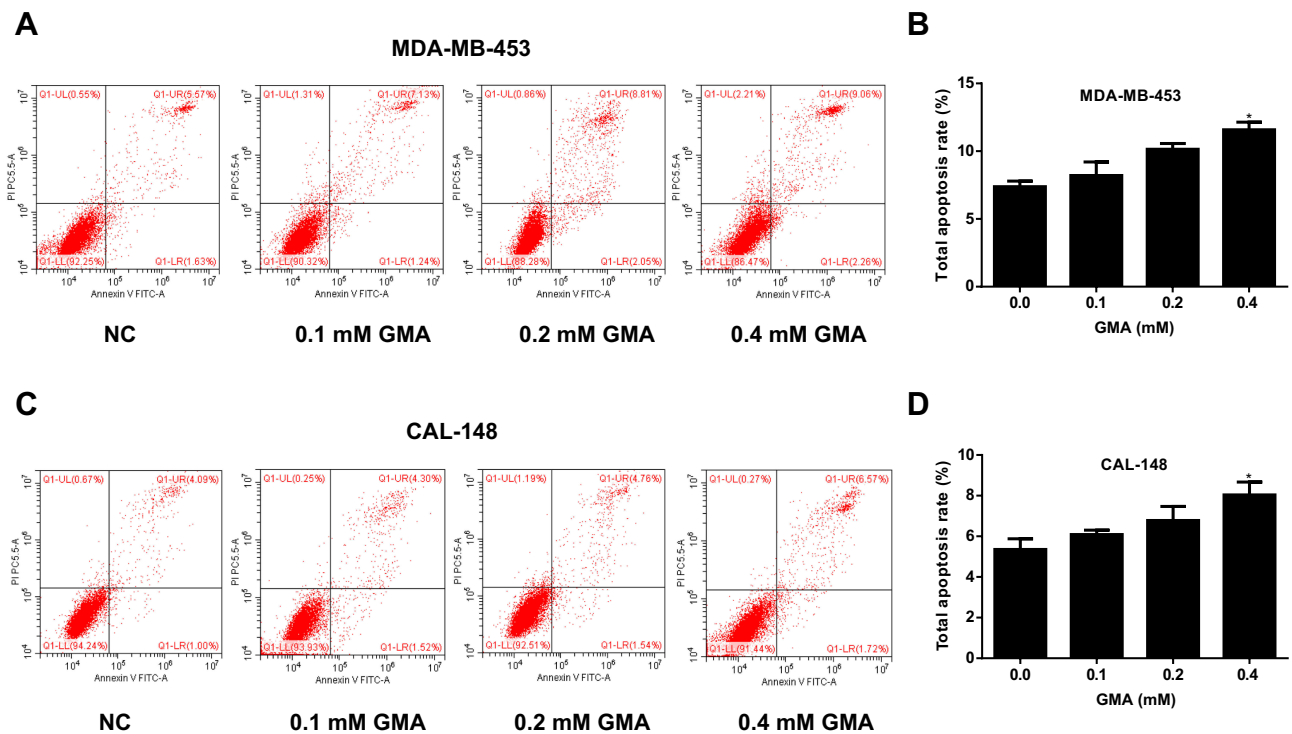
Figure 7 Effect of GMA on apoptosis of CAL-148 and MDA-MB-453 cells. (**A**) MDA-MB-453 cells were treated with different concentrations of GMA. After 48 h treatment, cells were harvested for flow cytometric analysis to detect cell apoptosis. (**B**) Quantitative cell apoptosis analysis results of MDA-MB-453 cells. (**C**) CAL-148 cells were treated with different concentrations of GMA. After 48 h treatment, cells were harvested for flow cytometric analysis to detect cell apoptosis. (**D**) Quantitative cell apoptosis analysis results of CAL-148 cells. *$p < 0.05$ versus the control group. N=3.
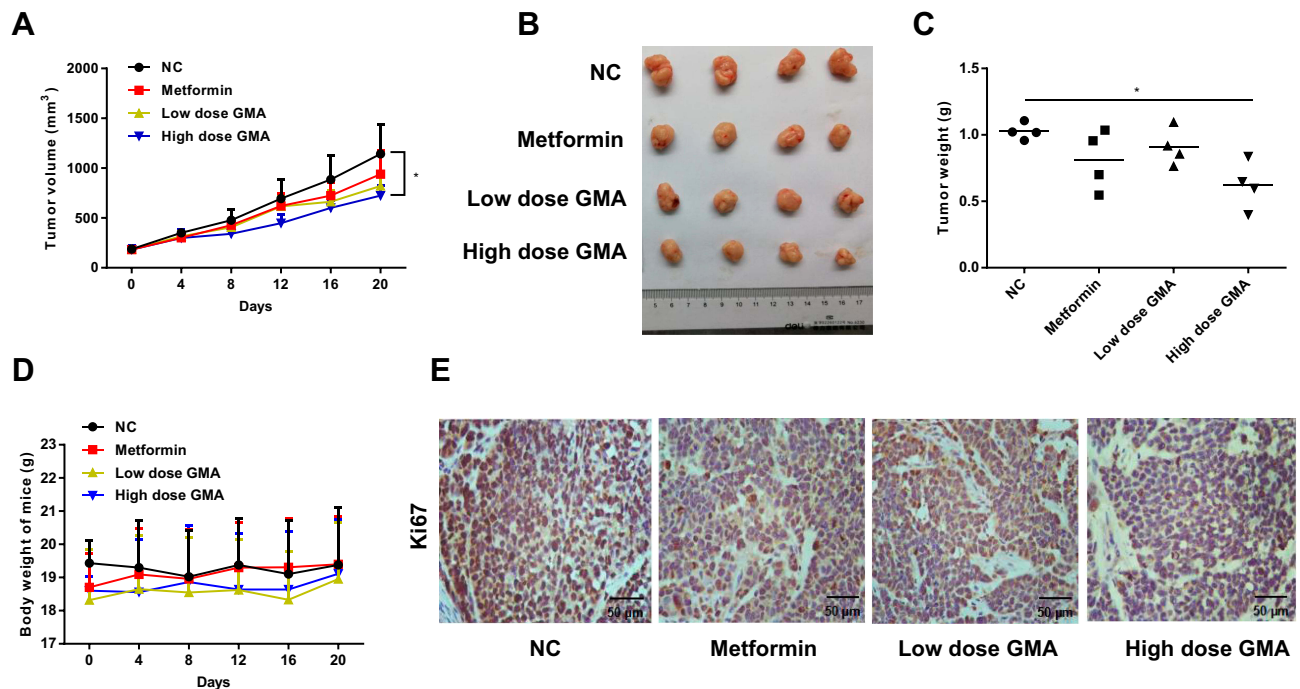

Figure 8 Effect of GMA on tumor growth in vivo. (**A**) Sixteen nude mice with CAL-148 xenografts were randomly divided into four groups (4 mice/group): the control group (15 mg/kg carboxymethyl cellulose), metformin group (200 mg/kg), low dose GMA group (200 mg/kg) and high dose GMA group (400 mg/kg) and daily administrated with the drugs as indicated by oral gavage for 3 weeks. Tumour volume and body weight of mice were measured every four days. The tumor growth curve was shown. *$p < 0.05$ versus the control group. (**B**) The image of the xenografts of each group. (**C**) The tumor weight of the xenografts of each group. *$p < 0.05$ versus the control group. (**D**) Body weight of mice of each group. (**E**) IHC analysis of Ki67 expression in the xenografts of each group. Representative images were shown. Magnification: 400×. Scale bar: 50μm.
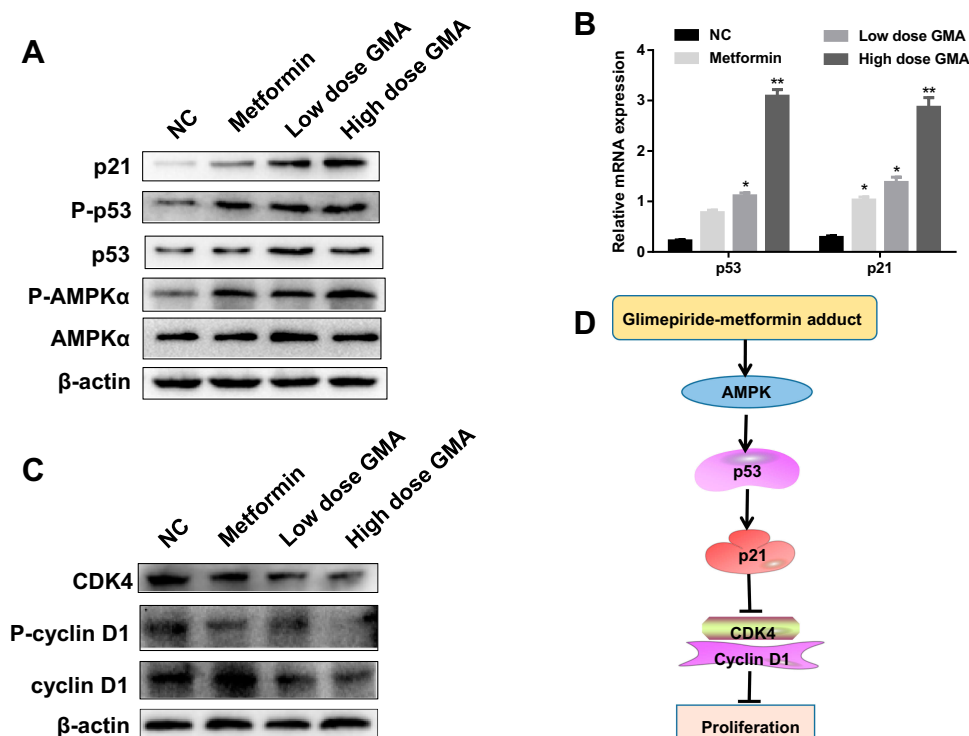
Figure 9 GMA activates AMPK and up-regulates the expression of p53 and p21. (**A**) Western blotting analysis of the protein levels of p-AMPKα, AMPKα, p-p53, p53 and p21 in the pooled extracts of xenografts in each group. β-actin was used as a loading control. N=3. Representative data were shown. (**B**) RT-qPCR analysis of relative mRNA expressions of p53, p21 in tumour tissues. Transcription levels were normalized to β-actin expressions. *$p < 0.05$ and **$p < 0.01$ versus the control group. (**C**) Western blotting analysis of the pooled extracts of the xenografts from each group. (**D**) The diagram of the proposed molecular mechanism of GMA action. GMA activates AMPK then up-regulates expression of p53 and p21 and suppresses cyclin D1 and CDK4 to induce cell cycle arrest, therefore, inhibiting the proliferation of breast cancer cells.

dose GMA group compared with the control group, implying that treatment with high dose GMA was safe (Figure 8D). Analysis of the proliferative index in tumor sections by immunohistochemistry revealed that high dose GMA significantly reduced the expression of Ki67, a proliferation marker of tumor, which further supports that high dose GMA suppresses breast cancer cell proliferation in vivo (Figure 8E).

GMA Activates AMPK and Up-Regulates P53 and P21 Expression

Studies have reported that Met achieves antineoplastic effects by activation of AMP-activated protein kinase (AMPK).[14–16] Therefore, we tested whether GMA inhibits breast cancer via activation of AMPK. Western blotting showed that phospho-AMPK levels were significantly increased in Met group, low dose GMA group and high dose GMA group, and high dose GMA group had highest levels of phospho-AMPK (Figure 9A). Next, we examined the expression of several crucial genes involving in cell cycle regulation relative to AMPK pathways. RT-qPCR and Western blotting showed that the expression levels

of p53 and p21 were obviously elevated in GMA-treated group compared with the control group (Figure 9A and B). Moreover, the levels of cyclin D1 and CDK4 were decreased (Figure 9C). Together, the above results suggest that GMA inhibits breast cancer cell proliferation through regulation of p53 and p21 expression via activation of AMPK (Figure 9D).

Discussion

Drug eutectic is a hot topic in the field of pharmacy in recent years. There are two kinds of eutectic crystals formed between two neutral solids, and there are also multiple eutectic crystals formed by neutral solids and salts or solvates. The eutectics are combined by hydrogen bonds or other non-covalent bond.[11,17] It has been confirmed that polymorphism and eutectic of drugs can seriously affect the clinical therapeutic effects, side effects and quality of drugs.[18–20] For example, LCZ696 is a supramolecular complex formed by eutectic technology with a 1:1 molar ratio of valsartan and shakabut. It is considered to be one of the most potential therapeutic drugs for chronic heart failure.[21] Levofloxacin and formyl

phenol form a kind of eutectic by stoichiometric ratio of 1:1, which can reduce the hygroscopicity of levofloxacin and improve its photostability.[22] GMA is a compound synthesized by glimepiride and metformin by a non-covalent bond at a molar molecular mass of 1:1. Infrared spectroscopy results show that GMA is integrated with glimepiride and metformin by hydrogen bonded, unlike the physical mixture of glimepiride and metformin hydrochloride, and it is shown that GMA is a new adduct.

Epidemiological studies have shown that metformin can reduce the incidence of cancer.[23] It has also been reported that glimepiride can inhibit MCF-7 breast cancer cell proliferation by regulating the expression of non-coding RNA.[24] In our study, we conducted preliminary explorations of the effects and mechanisms of GMA on anti-breast cancer cells. The results of in vitro experiments showed that GMA inhibited the proliferation of breast cancer cell lines MDA-MB-231, MCF-7, CAL-148, and MDA-MB-453. Among those breast cancer cell lines, CAL-148 and MDA-MB-453 cells were more sensitive to GMA. Moreover, we found that GMA can enhance effect of chemotherapy agents paclitaxel and cisplatin on breast cancer cells, especially when chemotherapy agents are used in low concentration. In vivo experiments showed that GMA suppressed the growth of CAL-148 xenografts.

AMPK is a cellular energy sensor found in all eukaryotic cells and plays an important role in lipid and glucose metabolism. It has been established that metformin can activate AMPK in tumor cells. Once activated, AMPK regulates tumor cell proliferation and metabolism by activating the catabolic pathway that distributes ATP.[25–27] In addition, AMPK induces a p53-dependent metabolic checkpoint and can stimulate p53-dependent G1 cell cycle arrest.[28] It has been reported that activation of AMPK can inhibit tumor growth by regulating p53 expression and activity in breast cancer.[29] p53 is a tumor suppressor gene, which arrests cell cycle, promotes cell apoptosis, inhibits tumor angiogenesis and so on.[30,31] In the cell cycle, the regulation of p53 is mainly reflected in the monitoring of G1 phase and G2/M phase correction points, which is closely related to transcriptional activation.[32] The p53 downstream gene p21 is a cyclin-dependent kinase inhibitor, and p21 binds to a series of Cyclin-CDK complexes, inhibiting the corresponding protein kinase activity and inducing G1 phase arrest.[33–35] In our study, we found that GMA activates AMPK, up-regulates expression of p53 and p21, and down-regulates expression of cyclin D1 and CDK4. Therefore, GMA might inhibit breast cancer proliferation through

activation of AMPK leading to cell cycle arrest. Interestingly, Mukhopadhyay S et al. have reported that 5-Aminoimidazole-4-carboxamide-1-β-4-ribofuranoside (AICAR), a metformin like antidiabetic drug and AMPK activator, affects breast cancer cell lines MDA-MB-231 and MCF-7 in a similar manner,[36] indicating that anti-breast cancer effect of antidiabetic drugs is not limited only in metformin or its derivatives. Why GMA is more potent to activate AMPK than metformin in tumors remains to be determined. It is worth mentioning that AMPK can also suppress mTORC1 via tuberous sclerosis complex 2 (TSC2) and/or the phospholipase D (PLD).[37] Suppression of mTOR could result in G1 cell cycle arrest.[38,39] As AMPK regulates mTOR pathways via PLD regulation,[37] and mTOR signaling plays a critical role in tumors, it will be interesting to investigate the effects of GMA on PLD activity and mTOR signaling.

In conclusion, our study suggests that GMA has a better anti-cancer effect than Gli and Met alone or combination at the same concentration. GMA inhibition of breast cancer cell proliferation might be through activation of AMPK leading to up-regulation of p53 and p21 and down-regulation of cyclin D1 and CDK4.

Disclosure

The authors report no conflicts of interest in this work.

References

1. Siegel Rebecca L, Miller Kimberly D, Ahmedin J. Cancer statistics, 2019. *CA Cancer J Clin*. 2019;69(1):7–34. doi:10.3322/caac.21551
2. Dent R, Trudeau M, Pritchard K, et al. Triple-negative breast cancer: clinical features and patterns of recurrence. *Clin Cancer Res*. 2007;13(15):4429–4434. doi:10.1158/1078-0432.CCR-06-3045
3. Harbeck N, Gnant M. Breast cancer. *Lancet*. 2017;389(10074):1134–1150. doi:10.1016/S0140-6736(16)31891-8
4. Maruthur N, Tseng E, Hutfless S, et al. Diabetes medications as monotherapy or metformin-based combination therapy for type 2 diabetes: a systematic review and meta-analysis. *Ann Intern Med*. 2016;164(11):740–751. doi:10.7326/M15-2650
5. Prateek S, Sanjeev K. Metformin inhibits human breast cancer cell growth by promoting apoptosis via a ROS-independent pathway involving mitochondrial dysfunction: pivotal role of superoxide dismutase (SOD). *Cell Oncol*. 2018;41(6):637–650. doi:10.1007/s13402-018-0398-0
6. Zhao Y, Zeng X, Tang H, Ye D, Liu J. Combination of metformin and paclitaxel suppresses proliferation and induces apoptosis of human prostate cancer cells via oxidative stress and targeting the mitochondria-dependent pathway. *Oncol Lett*. 2019;17(5):4277–4284. doi:10.3892/ol.2019.10119

7. Zheng Y, Zhu J, Zhang H, et al. Metformin inhibits ovarian cancer growth and migration in vitro and in vivo by enhancing cisplatin cytotoxicity. *Am J Transl Res*. 2018;10(10):3086–3098.

8. Ling S, Xie H, Yang F, et al. Metformin potentiates the effect of arsenic trioxide suppressing intrahepatic cholangiocarcinoma: roles of p38 MAPK, ERK3, and mTORC1. *J Hematol Oncol*. 2017;10 (1):59. doi:10.1186/s13045-017-0424-0

9. Yan X. Clinical efficacy of glimepiride tablets in the treatment of type 2 diabetes mellitus. *Diabetes New World*. 2017;20(23):109–110.

10. Du D, Wu C, Zou X, Lei X. The effect of glimepiride on the proliferation of human breast cancer cell MCF-7 by down-regulating miRNA-34a expression. *Chin Pharm*. 2019;22 (04):656–659.

11. Gao Y, Zu H, Zhang J. Progress in drug eutectic research. *Chem Prog*. 2010;22(5):829–836.

12. Liu Y, Hu X, Shan X, et al. Rosiglitazone metformin adduct inhibits hepatocellular carcinoma proliferation via activation of AMPK/p21 pathway. *Cancer Cell Int*. 2019;19(1):13. doi:10.1186/s12935-019-0732-2

13. Hu X, Bian X, Wang H, et al. An adduct and its preparation and use. China patent CN108299271A. 2018 July 20.

14. Zheng L, Yang W, Wu F, et al. Prognostic significance of AMPK activation and therapeutic effects of metformin in hepatocellular carcinoma. *Clin Cancer Res*. 2013;19(19):5372–5380. doi:10.1158/1078-0432.CCR-13-0203

15. Yi G, He Z, Zhou X, et al. Low concentration of metformin induces a p53-dependent senescence in hepatoma cells via activation of the AMPK pathway. *Int J Oncol*. 2013;43(5):1503–1510. doi:10.3892/ijo.2013.2077

16. Hur K, Lee MS. New mechanisms of metformin action: focusing on mitochondria and the gut. *J Diabetes Investig*. 2015;6(6):600–609. doi:10.1111/jdi.12328

17. Qiao N, Li M, Schlindwein W, et al. Pharmaceutical cocrystals: an overview. *Int J Pharm*. 2011;419(1–2):1–11. doi:10.1016/j.ijpharm.2011.07.037

18. Tong D, Hong M, Xu J, Zhao W, Ren G. Research progress and application of drug cocrystals. *Chin J Antibiot*. 2011;36(08):561–565.

19. Thipparaboina R, Thumuri D, Chavan R, et al. Fast dissolving drug-drug eutectics with improved compressibility and synergistic effects. *Eur J Pharm Sci*. 2017;104:82–89. doi:10.1016/j.ejps.2017.03.042

20. Haneef J, Chadha R. Drug-drug multicomponent solid forms: cocrystal, coamorphous and eutectic of three poorly soluble antihypertensive drugs using mechanochemical approach. *AAPS PharmSciTech*. 2017;18(6):2279–2290. doi:10.1208/s12249-016-0701-1

21. Mauro G, Michele S. Sacubitril/valsartan (LCZ696) for the treatment of heart failure. *Expert Rev Cardiovasc Ther*. 2016;14(2):145–153. doi:10.1586/14779072.2016.1128827

22. Shinozaki T, Ono M, Higashi K, et al. A novel drug-drug cocrystal of levofloxacin and metacetamol: reduced hygroscopicity and improved photostability of levofloxacin. *J Pharm Sci*. 2019;108(7):2383–2390. doi:10.1016/j.xphs.2019.02.014

23. Landman G, Kleefstra N, Van Hateren K, et al. Metformin associated with lower cancer mortality in type 2 diabetes: ZODIAC-16. *Diabetes Care*. 2010;33(2):322–326. doi:10.2337/dc09-1380

24. Fang Z, Liang J, Lu X. Downregulation of miRNA-214 expression by glimepiride inhibits proliferation of human breast cancer cell line MCF-7. *Chin Pharm*. 2018;1:14–17.

25. Viollet B, Guigas B, Sanz Garcia N, et al. Cellular and molecular mechanisms of metformin: an overview. *Clin Sci*. 2012;122 (6):253–270. doi:10.1042/CS20110386

26. Zhou G, Myers R, Li Y, et al. Role of AMP-activated protein kinase in mechanism of metformin action. *J Clin Invest*. 2001;108 (8):1167–1174. doi:10.1172/JCI13505

27. Mihaylova M, Shaw R. The AMP-activated protein kinase (AMPK) signaling pathway coordinates cell growth, autophagy, metabolism. *Nat Cell Biol*. 2011;13(9):1016–1023. doi:10.1038/ncb2329

28. Jones R, Plas D, Kubek S, et al. AMP-activated protein kinase induces a p53-dependent metabolic checkpoint. *Mol Cell*. 2005;18 (3):283–293. doi:10.1016/j.molcel.2005.03.027

29. Wang Z, Wang N, Liu P, et al. AMPK and Cancer. *Exp Suppl*. 2016;107:203–226. doi:10.1007/978-3-319-43589-3_9

30. Bykov Vladimir J, Eriksson Sofi E, Julie B, Wiman Klas G. Targeting mutant p53 for efficient cancer therapy. *Nat Rev Cancer*. 2018;18 (2):89–102. doi:10.1038/nrc.2017.109

31. Levine A, Oren M. The first 30 years of p53: growing ever more complex. *Nat Rev Cancer*. 2009;9(10):749–758. doi:10.1038/nrc2723

32. Basak D, Punganuru S, Srivenugopal K. Piperlongumine exerts cytotoxic effects against cancer cells with mutant p53 proteins at least in part by restoring the biological functions of the tumor suppressor. *Int J Oncol*. 2016;48(4):1426–1436. doi:10.3892/ijo.2016.3372

33. Abbas T, Dutta A. p21 in cancer: intricate networks and multiple activities. *Nat Rev Cancer*. 2009;9(6):400–414. doi:10.1038/nrc2657

34. Wang G, Fu Y, Hu F, et al. Loss of BRG1 induces CRC cell senescence by regulating p53/p21 pathway. *Cell Death Dis*. 2017;8 (2):e2607. doi:10.1038/cddis.2017.1

35. Georgakilas A, Martin O, Bonner W. p21: a two-faced genome guardian. *Trends Mol Med*. 2017;23(4):310–319. doi:10.1016/j.molmed.2017.02.001

36. Mukhopadhyay S, Chatterjee A, Kogan D, et al. 5-Aminoimidazole-4-carboxamide-1-β-4-ribofuranoside (AICAR) enhances the efficacy of rapamycin in human cancer cells. *Cell Cycle*. 2015;14 (20):3331–3339. doi:10.1080/15384101.2015.1087623

37. Mukhopadhyay S, Saqcena M, Chatterjee A, et al. Reciprocal regulation of AMP-activated protein kinase and phospholipase D. *J Biol Chem*. 2015;290(11):6986–6993. doi:10.1074/jbc.M114.622571

38. Saqcena M, Menon D, Patel D, et al. Amino acids and mTOR mediate distinct metabolic checkpoints in mammalian G1 cell cycle. *PLoS One*. 2013;8(8):e74157. doi:10.1371/journal.pone.0074157

39. Mukhopadhyay S, Saqcena M, Foster D. Synthetic lethality in KRas-driven cancer cells created by glutamine deprivation. *Oncoscience*. 2015;2(10):807–808. doi:10.18632/oncoscience.253